Molecular Biology of the Cell
Vol. 18, 2579–2591, July 2007

Ena/VASP Proteins Have an Anti-Capping Independent Function in Filopodia Formation[D] [V]

Derek A. Applewhite,* Melanie Barzik,† Shin-ichiro Kojima,* Tatyana M. Svitkina,‡ Frank B. Gertler,† and Gary G. Borisy*§

*Department of Cell and Molecular Biology, Feinberg School of Medicine, Northwestern University, Chicago, IL 60611; †Department of Biology, Massachusetts Institute of Technology, Cambridge, MA 02139; ‡Department of Biology, University of Pennsylvania, Philadelphia, PA 19104; and §Marine Biological Laboratory, Woods Hole, MA 02453

Submitted November 6, 2006; Revised March 28, 2007; Accepted April 24, 2007
Monitoring Editor: David Drubin

Filopodia have been implicated in a number of diverse cellular processes including growth-cone path finding, wound healing, and metastasis. The Ena/VASP family of proteins has emerged as key to filopodia formation but the exact mechanism for how they function has yet to be fully elucidated. Using cell spreading as a model system in combination with small interfering RNA depletion of Capping Protein, we determined that Ena/VASP proteins have a role beyond anticapping activity in filopodia formation. Analysis of mutant Ena/VASP proteins demonstrated that the entire EVH2 domain was the minimal domain required for filopodia formation. Fluorescent recovery after photobleaching data indicate that Ena/VASP proteins rapidly exchange at the leading edge of lamellipodia, whereas virtually no exchange occurred at filopodial tips. Mutation of the G-actin–binding motif (GAB) partially compromised stabilization of Ena/VASP at filopodia tips. These observations led us to propose a model where the EVH2 domain of Ena/VASP induces and maintains clustering of the barbed ends of actin filaments, which putatively corresponds to a transition from lamellipodial to filopodial localization. Furthermore, the EVH1 domain, together with the GAB motif in the EVH2 domain, helps to maintain Ena/VASP at the growing barbed ends.

INTRODUCTION

Actin-based protrusions known as filopodia, first described by Porter, Claude, and Fullam as early as 1945 (Porter *et al.*, 1945; Albrecht-Buehler, 1976), are composed of tightly bundled parallel filaments 5–50 μm long and 0.1–0.5 μm thick (Small, 1988; Mitchison and Cramer, 1996). Filopodia have been implicated in a number of cellular processes including neuronal growth cone pathfinding, embryonic development, wound healing, and metastasis (Jacinto *et al.*, 2000, 2001; Vasioukhin and Fuchs, 2001; Dent and Gertler, 2003; Hashimoto *et al.*, 2005). Despite the importance of filopodia to so many diverse cellular functions, the exact mechanism governing their initiation and formation has yet to be fully explained. A number of actin-binding proteins have been implicated in the formation of filopodia, most recently myosin X and the formin family of proteins, which catalyze the formation of long unbranched actin filaments (Evangelista *et al.*, 2003; Zigmond, 2004; Bohil *et al.*, 2006; Kovar, 2006). However, in several cell types, filopodia and the sheet-like Arp2/3-based lamellipodia, rapidly interchange during protrusion, suggesting commonalities between the two structures (Svitkina *et al.*, 2003). The type of protrusion that dominates in the subcellular compartment critically depends on whether filaments are allowed to elongate persistently or are capped shortly after nucleation. Accordingly, when the heterodimeric Capping Protein (CP), the major barbed end terminator in lamellipodia, is silenced by small interfering RNA (siRNA), the balance between the two structures, is shifted to favor filopodial formation (Mejillano *et al.*, 2004). A similar phenomenon has been observed in vitro where a decrease in CP levels led to a transition from a dendritic-like network reminiscent of lamellipodia to a bundled filopodial-like actin organization (Vignjevic *et al.*, 2003; Haviv *et al.*, 2006).

Although it appears that CP levels determine which actin-based protrusive organelle dominates at the cell periphery, it does not function in isolation. The Ena/VASP family of proteins, which includes three mammalian homologues, Mena (Mammalian Enabled), VASP (Vasodilator-Stimulated Phosphoprotein), and EVL (Ena-VASP-Like), also influence the underlying actin architecture (Waldmann *et al.*, 1987; Reinhard *et al.*, 1992; Gertler *et al.*, 1995, 1996; Bear *et al.*, 2002). By cellular localization alone, Ena/VASP proteins appear to be vital to this lamellipodial-filopodial transition because they localize to both the leading edge of protruding lamellipodia as well as filopodial tips (Reinhard *et al.*, 1992; Gertler *et al.*, 1996; Lanier *et al.*, 1999; Rottner *et al.*, 1999). Recent work in neuronal cells demonstrates the crucial role Ena/VASP proteins have in filopodia formation. Targeting of Ena/VASP proteins to the inner leaflet of the cell membrane led to an increase in the number and length of filopodia in primary hippocampal neurons. Conversely, sequestration of Ena/VASP proteins to mitochondria led to decreased filopodia formation and inhibition of filopodia induction upon treatment with the neuronal guidance fac-

This article was published online ahead of print in *MBC in Press* (http://www.molbiolcell.org/cgi/doi/10.1091/mbc.E06–11–0990) on May 2, 2007.

[D] [V] The online version of this article contains supplemental material at *MBC Online* (http://www.molbiolcell.org).

Address correspondence to: Gary G. Borisy (gborisy@mbl.edu).

tors Netrin-1 or forskolin (Lebrand *et al.*, 2004). Similarly, in *Dictyostelium*, genetic ablation of dVASP, the sole Ena/VASP member present in the organism, decreased filopodia formation and caused chemotactic defects (Han *et al.*, 2002). Finally, experimental evidence demonstrates that the lamellipodial-to-filopodial transition that occurs upon depletion of CP requires Ena/VASP proteins. Depletion of CP in cells lacking VASP and Mena and containing only trace amounts of EVL caused the cells to lose their ability to robustly form filopodia. The reintroduction of a single Ena/VASP member at physiological levels was needed to recapitulate the hyper-filopodial phenotype that occurs upon CP depletion (Mejillano *et al.*, 2004).

Whereas experimental evidence supports a positive role for Ena/VASP proteins in filopodia formation, a clear mechanism of how they are involved in the process has yet to be elucidated. Biochemically, Ena/VASP proteins have been shown to antagonize filament termination, thereby increasing the length of actin filaments; however, the anti-capping function of Ena/VASP is still a point of controversy in the field and some investigators have reported otherwise (Bearer *et al.*, 2000, 2002; Samarin *et al.*, 2003; Barzik *et al.*, 2005; Schirenbeck *et al.*, 2006). Ena/VASP can bind to both barbed ends and sides of actin filaments through G-actin binding (GAB) and F-actin binding (FAB) motifs, respectively, that are harbored within the C-terminal EVH2 domain. Additionally, through a coiled-coil (COCO) domain at the extreme C-terminus, Ena/VASP forms tetramers (Huttelmaier *et al.*, 1999; Walders-Harbeck *et al.*, 2002; Zimmermann *et al.*, 2002; Krause *et al.*, 2003; Kuhnel *et al.*, 2004; Barzik *et al.*, 2005). Ena/VASP proteins are targeted to sites of dynamic actin turnover including focal adhesions, lamellipodial and filopodial tips, and ActA of *Listeria monocytogenes*, via their N-terminal EVH1 domain, which binds the consensus sequence D/E FPPPPXD/E (Chakraborty *et al.*, 1995; Niebuhr *et al.*, 1997; Carl *et al.*, 1999; Fedorov *et al.*, 1999; Laurent *et al.*, 1999). Through a central poly-proline domain, Ena/VASP binds to profilin, and to SH3 and WW domain–containing proteins (Gertler *et al.*, 1996; Ermekova *et al.*, 1997; Ahern-Djamali *et al.*, 1999; Krause *et al.*, 2003). Thus, Ena/VASP proteins possess the requirements needed for filopodia formation through the antagonism of CP and oligomerization of actin filaments and serve as adapter proteins for the assembly of multiprotein complexes for putative interactions with a number of actin-binding proteins.

Given the multidomain organization of the proteins it is likely that Ena/VASP proteins are involved in several steps in the filopodia initiation and formation process. If Ena/VASP proteins functioned only to antagonize barbed end capping as suggested initially, then under the conditions where CP is depleted, the necessity for Ena/VASP proteins in filopodia formation would be eliminated. Continuous elongation of actin filaments is a necessary, but not sufficient condition for filopodia formation. If actin filaments remain uncapped and continue to elongate, it is likely that the force generated by the growing filaments would be insufficient to effectively push against the membrane because of the intrinsic flexibility of long actin filaments (Mogilner and Edelstein-Keshet, 2002; Pollard and Borisy, 2003; Mogilner and Rubinstein, 2005). Therefore, Ena/VASP proteins may also function to aggregate or cross-link actin barbed ends to provide stability and create force. The fact that Ena/VASP proteins have been shown to bundle actin filaments supports this hypothesis, and the C-terminal tetramerization domain of Ena/VASP provides an additional tool for bringing barbed ends into close proximity (Bachmann *et al.*, 1999; Huttelmaier *et al.*, 1999; Laurent *et al.*, 1999; Bearer *et al.*, 2000; Kuhnel *et al.*, 2004; Barzik *et al.*, 2005). This initial aggregation of actin filaments could potentially play an additional role in recruiting actin bundling proteins such as fascin that bundle parallel actin filaments (Svitkina *et al.*, 2003; Vignjevic *et al.*, 2003, 2006). Finally, the simultaneous binding of G-actin and profilin Ena/VASP proteins could sequester actin monomers primed for polymerization to the tips of filopodia where the barbed ends are located (Harbeck *et al.*, 2000; Chereau and Dominguez, 2006).

To test the specific mechanisms of Ena/VASP proteins in filopodia formation and to determine which domain or domains are necessary to this function, we analyzed various mutants of Ena/VASP in a mouse fibroblastic MV^{D7} cell line. The MV^{D7} line was generated from a VASP/Mena double-knockout mouse expressing only trace amounts of EVL. Therefore reintroduced wild-type or mutant Mena/VASP could be analyzed in the virtual absence of the three mammalian Ena/VASP family members (Bear *et al.*, 2000; Geese *et al.*, 2002; Loureiro *et al.*, 2002). Though lamellipodial protrusion and *Listeria* movement were well characterized in this system, filopodia formation has not been documented. One of the difficulties in analyzing filopodia formation in the MV^{D7} cell lines is that the cells do not robustly make filopodia once fully spread and are less protrusive in comparison to other cell lines. In this work, we overcame this obstacle by observing the cells during the spreading phase. Furthermore, we adopted the method of RNA interference of CP to decrease the barbed end termination of actin filaments within the lamellipodia. This approach allowed us to answer the question of whether Ena/VASP proteins act only to antagonize the capping activity by CP or play additional roles in filopodia formation. Through detailed analysis, we concluded that the EVH2 domain is the minimal domain needed to enhance filopodia formation. Furthermore, any defect to the GAB, FAB, or COCO domains found within the EVH2 domain compromised the ability of filopodia induction even under conditions where CP was depleted. These results indicate a novel role of Ena/VASP in filopodia formation beyond bundling, as suggested for dVASP (Schirenbeck *et al.*, 2005). An additional question is how to reconcile the differences in Ena/VASP function based on dual localization in both lamellipodia and filopodia. Through fluorescent recovery after photobleaching (FRAP) analysis we discovered a dramatic change of molecular dynamics of Ena/VASP associated with a transition from lamellipodial leading edge localization to filopodial tips. Finally, results from FRAP analysis also indicate the importance of the G-actin–binding domain to the stabilization of Ena/VASP at actin barbed ends.

MATERIALS AND METHODS

Expression Plasmids

The pDsRed-Super small hairpin RNA (shRNA) vector was constructed by replacing GFP cDNA from pG-Super (Kojima *et al.*, 2004) with DsRed2 cDNA from pDsRed2-N1 (Clontech, Palo Alto, CA) using SacII-NotI sites. The EVH1-only (amino acid residues 1–113) and EVH2-only (residues 225–340) fragments were PCR-amplified from human VASP gene and subcloned into pEGFP-N1 vector (Clontech) using Bam H1-XhoI sites. pmCherry-Actin was constructed from transferring human β-actin cDNA from pEGFP-Actin (Clontech) to pmCherry-C1 (Vignjevic *et al.*, 2006). pEGFP-VASP and pmCherry-fascin are described elsewhere (Vignjevic *et al.*, 2006).

Cell Culture and Microscopy

MV^{D7} VASP derivative cell lines including VASP EVH2, VASPΔFAB, VASPΔCOCO, VASP EVH2-ΔFAB, VASP EVH2-ΔCOCO, VASP GAB mutant (R232E,K233E), VASP(S153A), VASP (S235A,S274A), and VASP (S153A, S235A,S273A) were generated as previously described (Loureiro *et al.*, 2002) and MV^{D7} cells including VASP and Mena derivative cell lines (Mena EVH2,

Mena [S236A,S376A], Mena [S236D,S376D], MenaΔPRO, MenaΔFAB, MenaΔCOCO; Loureiro *et al.*, 2002) and were cultured as described (Bear *et al.*, 2000). B16F1 mouse melanoma cells were provided by C. Ballestrem (Weizmenn Institute of Science) and were maintained as previously described (Ballestrem *et al.*, 1998). COS7 green monkey kidney cells were obtained from ATCC (Manassas, VA) and maintained in DMEM supplemented with 10% fetal bovine serum (FBS). Transfection was performed using TransIT-LT1 (Mirrus, Boston, MA) for MV^{D7} lines and COS7, or FuGENE6 (Roche, Indianapolis, IN) for B16F1 according to manufacturer's recommendations.

Light microscopy was performed using an inverted microscope (Eclipse TE2000 or Diaphot 300, Nikon, Melville, NY) equipped with a plan 100× 1.3 NA objective and a back-illuminated cooled CCD camera (model CH250 and CH350, Roper Scientific, Tucson, AZ) driven by Metamorph imaging software (Universal Imaging, West Chester, PA). Live cell imaging of MV^{D7} cell lines was carried out in L-15 media containing recombinant mouse γ-interferon (Invitrogen, Carlsbad, CA; 10^6 units/ml) and 15% FBS. For live cell imaging of B16F1, cells were transferred to L-15 supplemented with 10% FBS. During live cell imaging, the microscope stage was maintained at ~37°C for B16F1 or at 32°C for MV^{D7} derivative cell lines.

Immunofluorescence

Immunostaining for CP was performed by treating cells for 5 min with 1% Triton X-100 in PEM buffer (100 mM Pipes, pH 6.9, 1 mM $MgCl_2$, 1 mM EGTA) containing 2% PEG MW 40,000 (Serva, Paramus, NJ) and 2 μM phalloidin, followed by fixation by 0.2% glutaraldehyde in 100 mM coxyladilic acid and quenching with $NaBH_4$. Anti-CPβ antibodies were obtained from D. Schafer (University of Virginia). Immunostaining for Arp2/3 complex and lamellipodin was performed by fixing cells with 4% paraformaldehyde, followed by permeating with 1% Triton X-100. The rabbit polyclonal Arp 3 antibody was purchased from Upstate Biotechnology (Lake Placid, NY) and the rabbit polyclonal anti-lamellipodin was previously prepared in Krause *et al.* (2004). Immunostaining for antiphosphorylated tyrosine (4G10, Upstate Biotechnology) was performed by simultaneously extracting with 0.5% Triton X-100 and fixing with 0.25% glutaraldehyde in PEM buffer, followed by fixation in 0.2% glutaraldehyde in 100 mM coxyladilic acid and quenching with $NaBH_4$. Immunostaining for fascin was performed by methanol fixation at −20°C. The mouse monoclonal antibody (clone 55K-2) was purchased DakoCytomation (Fort Collins, CO). TRITC-conjugated anti-rabbit IgG and anti-mouse IgG were purchased from Jackson ImmunoResearch (West Grove, PA). F-actin was stained with 0.033 μM of AlexaFlour350-Texas Red-X-, or AlexaFlour647-phalloidin (Molecular Probes, Eugene, OR).

Cell-spreading Assay

The cell-spreading assay was performed by trypsinizing (0.05% trypsin and 0.53 mM EDTA) MV^{D7} cells and replating them on laminin (20 μg/ml)-coated coverslips. Cells were allowed to attach and spread for ~10–15 min and then were imaged for ~20–40 min or until cells were fully spread. Transfected cells (containing the shRNA vector targeted against CPβ) were identified by DsRed2-soluble marker by epifluorescence, whereas imaging and phenotyping was done by phase-contrast microscopy.

FRAP Analysis

FRAP experiments were performed on a Zeiss LSM 510 confocal microscope (Carl Zeiss, Oberkochen, Germany) with a 110×/1.3 NA planapochromat oil objective and an argon laser (1 mW). B16F1 mouse melanoma cell or MV^{D7} fibroblast were maintained at 37 or 32°C, respectively. Enhanced green fluorescent protein (EGFP)-tagged full-length VASP or the EVH1 domain from VASP were transiently expressed B16F1 cells, whereas EGFP-EVH2 (VASP) was analyzed in MV^{D7} cells after transient transfection. For analysis of mutant Ena/VASP proteins, MV^{D7} derivatives stably expressing EGFP-VASP mutants were used. Cells were bleached by defining a rectangular region (8–15 μm^2) perpendicular to the direction of protrusion or at the filopodia tips (2–8 μm^2) for ~1 s using the 488-nm laser line at 100% laser power (25 mW). Subsequent GFP fluorescent images were acquired at ~0.5–3-s intervals with the excitation line of the 4880-nm laser line and phase images by a halogen light source. The Co-FRAP experiments were performed sequentially in the multitrack mode using both a 488-nm line from a 25-mW Argon laser and the 543-nm line from a 5-mW helium-neon laser at 100% power for bleaching of EGFP-VASP and mCherry-actin, respectively. B16F1 cells transfected with pEGFP-VASP and pmCherry-Actin plasmids were used. A 4–10-μm^2 rectangular region was bleached the distal portion of a protruding filopodium. Subsequent EGFP, mCherry, and phase images were acquired at 0.5–3-s intervals with 488- and 543-nm laser lines and halogen light, respectively.

The obtained images were analyzed by Metamorph software (Universal Imaging). EGFP-tagged protein fluorescent intensities were measured in the bleach zone in each frame. The loss of fluorescent intensity due to photofading was determined as follows: fluorescent intensity in a nonbleached region was measured over time and was fitted to an exponential decay function, $\exp(-k_{fade}t)$, where k_{fade} is the decay constant and t is time. The intensity of the bleach zone was corrected for photofading by multiplying a correction factor, $\exp(k_{fade}t)$ at each time point. The corrected fluorescent recovery intensities were then curved fitted using the expression $I(t) = I_f + (I_{PB} - I_f)\exp(-k_{rec}t)$, where I(t) = intensity at final time, I_{PB} = intensity at photobleaching event, and k_{rec} = fluorescence recovery rate constant. Half-time of recovery time was calculated as $\ln 2/k_{rec}$.

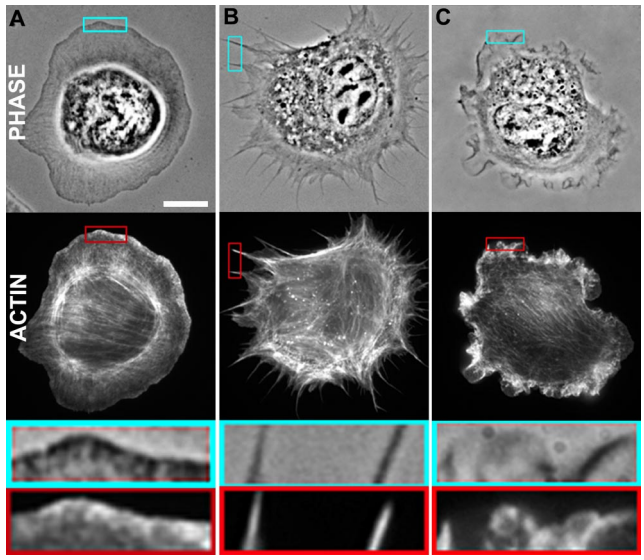

Figure 1. Three characteristic spreading phenotypes. Phase-contrast (phase) and phalloidin-stained (actin) images. (A) Smooth-Edged phenotype. Characterized by a flat, evenly spreading leading edge (phase) enriched in actin as visualized by phalloidin staining. Scale bar, 10 μm. (B) Filopodial phenotype. Characterized by long actin-containing protrusions. (C) Ruffling phenotype. Characterized by phase-dense undulations with corresponding actin-rich regions.

RESULTS

MV^{D7} Cells Have Three Distinct Spreading Modes

To study protrusion we used cell spreading as a model system. Spreading cells are particularly protrusive and have many characteristics general to migrating cells (Dubin-Thaler *et al.*, 2004). MV^{D7} mouse fibroblasts, parental or derivative, have three different spreading modes: Smooth-Edged, Filopodial, or Ruffling (Figure 1, A–C). Cells with the Smooth-Edged phenotype are characterized by a "fried-egg"-like appearance in phase microscopy, expanding evenly at the perimeter (Figure 1A). Wide-field fluorescence microscopy reveals an outer perimeter characteristic of protruding lamellipodia with increased fluorescence intensity after phalloidin staining. The Filopodial phenotype (Figure 1B) is characterized by filopodia, dynamic finger-like protrusions, which elongate as the cell spreads a hallmark of genuine filopodia. In addition, these filopodia contain actin along the shaft (Figure 1B). The Ruffling phenotype (Figure 1C) was defined by phase-dense wave-like structures, usually undergoing cycles of protrusion and retraction throughout the time of spreading. The phase-dense regions were enriched in actin as revealed by phalloidin staining. Time-lapsed movies demonstrate that different phenotypes were likely a result of a dynamic, protrusive process rather than retraction (Supplementary Movies 1–3). These three phenotypes represent the intrinsic heterogeneity of the MV^{D7} and derivative cell lines during spreading and were used to characterize the protrusive behavior of cells depending on the presence of individual Ena/VASP proteins.

Characterization of Smooth-Edged and Filopodial Phenotypes

The two spreading phenotypes, Smooth-Edged and Filopodial, were further defined in terms of the localization of

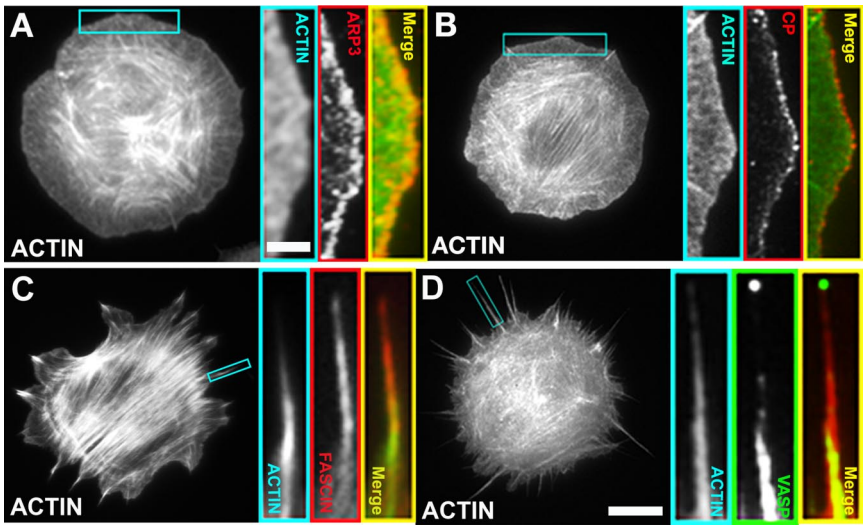

Figure 2. Lamellipodial and filopodial markers in spreading cells. Low magnification images show actin distribution. Scale bar, 10 μm. High magnification images of boxed regions are presented to the right of the low magnification images. Scale bar, 2 μm. (A) Higher magnification of actin distribution (cyan), Arp 2/3 complex localized by immunostaining for Arp 3 (red), and a merge of the actin and Arp2/3 distributions (yellow) in a cell in the Smooth-Edged spreading phenotype. Arp 2/3 present at the spreading edge of the lamellipodia. (B) Actin distribution at high magnification (cyan), CP localized by immunostaining for the CPβ subunit (red) and a merged image of the actin and CP distributions (yellow) in a cell in the Smooth-Edged spreading phenotype. CP is present at the spreading edge of the lamellipodia. (C) Actin distribution at high magnification (cyan), fascin localized by expression of mCherry-fascin (red), and a merged image of actin and fascin (yellow) in a cell in the Filopodial spreading phenotype. Fascin colocalized with F-actin bundles present along the length of filopodia. (D) Actin distribution along the length of a filopodium (cyan), VASP localized by expression of EGFP-VASP in MV^{D7}-VASP stable cell line (green), and the combination of actin and VASP distributions in the merged image (yellow) of a cell in the Filopodial phenotype. VASP is accumulated at tips of filopodia.

lamellipodial and filopodial markers. Two lamellipodial proteins required for the generation of protrusion, the Arp2/3 complex and heterodimeric CP (Schafer *et al.*, 1998; Svitkina and Borisy, 1999; Pollard *et al.*, 2000), showed localization to the extreme cell periphery (Figure 2, A and B), a subcellular localization observed in the lamellipodia of fully spread cells. These results demonstrate that the protrusive structures of cells in the Smooth-Edged phenotypical category are lamellipodia.

We differentiated between filopodial and lamellipodial modes of protrusion using the filopodial markers, fascin, and VASP. We transiently expressed mCherry-fascin in spreading MV^{D7}-VASP cells and observed that fascin localized to the shaft of the finger-like protrusions (Figure 2C). Additionally, we observed EGFP-VASP, a canonical molecular marker of filopodia, at the tips of actin-containing protrusions (Figure 2D) (Han *et al.*, 2002; Krause *et al.*, 2003; Kwiatkowski *et al.*, 2003; Svitkina *et al.*, 2003). On the basis of these results and considering their protrusive behavior, we conclude that the actin-based protrusions characteristic of the Filopodial phenotypical category are genuine filopodia.

Contribution of Ena/VASP Protein Domains during Filopodia Formation

The above results ensured the feasibility of the spreading assay for analysis of filopodia formation. We sought to determine how the various domains of Ena/VASP proteins contribute to filopodia formation by using the cell-spreading assay. We analyzed the frequency of the Smooth-Edged, Filopodial, and Ruffling phenotypes occurring in the MV^{D7} derivative cell lines by phase-contrast live-cell imaging (Figure 3A). It was during this highly dynamic, protrusive pe-

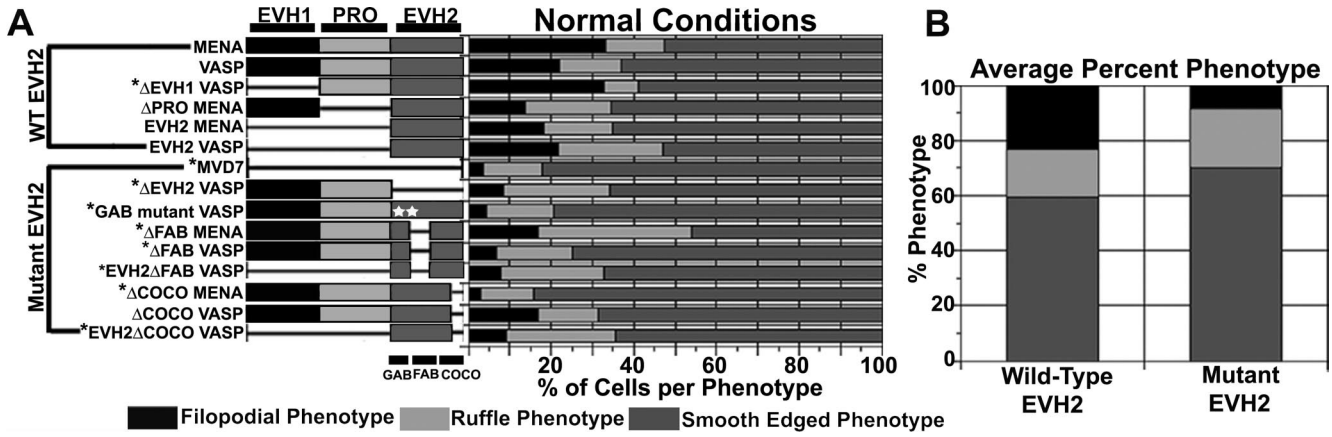

Figure 3. Cell-spreading assay, under normal conditions. In the cell-spreading assay, phenotypes were assessed by phase-contrast microscopy in live cells during the spreading phase (see *Materials and Methods* for detail). (A) The schematic diagram of the mutated/deleted Ena/VASP proteins represents the cell lines used in the assay. These proteins were stably expressed as EGFP-tagged form in MV^{D7} fibroblasts using retroviral vectors. The bar graph depicts percentage of cells displaying Smooth-Edged, Filopodial, and Ruffling phenotypes for each cell line. (B) The column bar graph represents the average percentages of the Smooth-Edged, Filopodial, and Ruffling phenotypes for groups containing or lacking wild-type EVH2 given in A. The average percentages of the three phenotypes in the EVH2-containing group were used for χ^2-test for each line. The asterisks in A indicate statistical significance ($p < 0.05$).

riod that the cells were scored and binned into one of the phenotypic categories. It is important to note that the initial observations were made during a finite period of cell spreading and therefore that we cannot exclude the possibility that the cells may have switched spreading modes once this period of data acquisition ended. The tested mutants (Figure 3A) included deletion of the EVH1, Proline-rich (PRO), and/or EVH2 domain(s). In addition, we dissected the EVH2 domain in more detail using mutations of the GAB motif (R232E, R233E) and deletion of the FAB or COCO motif. The GAB motif of mammalian Ena/VASP proteins share close homology with that of the β-thymosin family of proteins, and it is thought that the G-actin–binding site is needed to mediate the formation of a complex between Ena/VASP, profilin-actin, and actin filament barbed ends (Harbeck *et al.*, 2000; Walders-Harbeck *et al.*, 2002; Barzik *et al.*, 2005). It is likely that this complex formation would support positioning and maintenance of Ena/VASP proteins at filopodial tips. Point mutations at key positive residues have been shown to ablate the ability of these proteins to bind G-actin (Huttelmaier *et al.*, 1999; Harbeck *et al.*, 2000; Walders-Harbeck *et al.*, 2002). We infected MV^{D7} cells with retroviruses for EGFP-tagged VASP or Mena mutants and used FACS to select cells with a certain range of expression level of EGFP-fusion proteins. Therefore differences the in expression level among a series of mutants was virtually negligible.

We observed that the Smooth-Edged spreading phenotype dominated regardless of how the Ena/VASP protein was mutated or deleted. However, a closer analysis revealed that the Filopodial mode was elevated in the group of cell lines with an intact or wild-type EVH2 domain (MV^{D7}-Mena, MV^{D7}-VASP, MV^{D7}-ΔEVH1 (VASP), MV^{D7}-ΔPRO (Mena), MV^{D7}-EVH2 (Mena), and MV^{D7}-EVH2 (VASP) compared with the other group with deletions or mutations to the EVH2 domain (parental MV^{D7} cell line, MV^{D7}-ΔEVH2, MV^{D7}-GAB mutant, MV^{D7}-ΔFAB (Mena), MV^{D7}-ΔFAB (VASP), MV^{D7}-EVH2ΔFAB (VASP), MV^{D7}-ΔCOCO (VASP), MV^{D7}-ΔCOCO (Mena), and MV^{D7}-EVH2ΔCOCO (VASP) (Figure 3A). To quantify the differences between these two groups, we performed a χ^2-test. We determined the average percentages of the Smooth-Edged, Filopodial, and Ruffling categories within the wild-type EVH2 group and compared these expected values to the observed percentages of the three phenotypic categories for each individual cell line used in the assay (Figure 3, A and B). The results of the χ^2-test are given in Figure 3A; in general the mutant EVH2 group was statistically significantly different ($p < 0.05$) from the wild-type EVH2 group as indicated by asterisks. The two exceptions were the MV^{D7}-ΔEVH1 (VASP) and MV^{D7}-ΔCOCO (VASP) cell lines. Given that the χ^2-test determines statistical significance based on the frequency of phenotypes these two cell lines varied slightly from their respective groups in the frequency of cells in the Ruffling and Filopodial modes, correspondingly. Collectively, the results from the spreading assay imply that even under normal conditions, Ena/VASP proteins impart differences on spreading modes, increasing the frequency at which filopodia from, yet deletions or mutations of the EVH2 domain lead to increased frequency of Ruffling. Despite the differences between cell lines containing wild-type EVH2 and mutant EVH2 domains, the majority of cells from both groups spread by the Smooth-Edged mode. Thus, we needed a better tool to study Ena/VASP proteins in filopodia formation.

The EVH2 Domain of Ena/VASP Proteins Is Required to Promote Filopodia Formation in the Absence of Capping Protein

Although biochemical data indicates that Ena/VASP proteins function as an antagonist for filament termination, presumably this is not their only role in filopodia formation. To test the functions of Ena/VASP proteins beyond anticapping activity in filopodia formation, we depleted CP, which is the major barbed end terminator, using a plasmid-based shRNA mammalian expression vector and performed the cell-spreading assay. The hairpin RNA expression plasmid contains a DsRED2 expression cassette that allowed us to identify knockdown by red fluorescence. CP depletion led to a robust increase in the Filopodial spreading phenotype in the wild-type EVH2 group, increasing from an average frequency of 24% in non–CP-depleted cells to over 60% in CP-depleted cells (Figure 4, A and B). A similar robust change occurred in the mutant EVH2 group, however, instead of an increase in the Filopodial phenotype, CP depletion increased the frequency of Ruffling cells from 21 to over

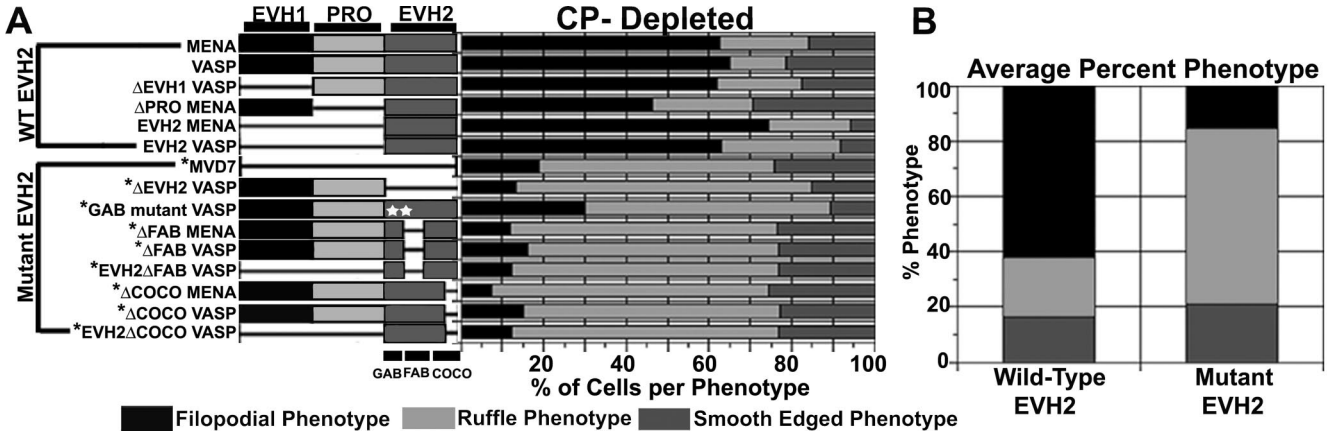

Figure 4. Cell-spreading assay, CP-depleted. MV^{D7} and derivative cell lines were transfected with CPβ-depleting plasmid (pDsRed-SUPER-CPβ-T1), which expressed DsRed2 marker and shRNA against CPβ simultaneously. Four days after transfection, the phenotypes were assessed as in Figure 3. Transfectants were identified by DsRed-soluble marker. (A) The schematic diagram of the mutated/deleted Ena/VASP protein and the bar graph of the percentages of the Smooth-Edged, Filopodial, and Ruffling phenotypes. (B) The average percentages of the three phenotypic categories for the wild-type and mutant groups of MV^{D7} derivative cell lines given in A. The asterisks indicate statistically significant difference ($p < 0.01$, χ^2-test) from the average of the wild-type group.

Table 1. Ena/VASP phosphorylation mutants

Ena/VASP protein	% Smooth-edged		% Filopodial		% Ruffles	
	Non-CP depleted	CP-depleted	Non-CP depleted	CP-depleted	Non-CP depleted	CP-depleted
Mena (S236D, S376D)	60	20	16	57	24	23
Mena (S236A, S376A)[a]	67	8	10	20	24	72
VASP (S153A)[a]	55	14	25	38	20	48
VASP (S235A, T274A)[a]	65	13	20	43	15	44
VASP (S153A, S235A, T274A)[a]	58	10	27	47	15	43

[a] Significantly different from cells with wild-type EVH2 domains; $p < 0.01$; χ^2-test.

60%. Both groups underwent a concomitant decrease in the Smooth-Edged phenotype after CP depletion (Figure 4, A and B).

The χ^2-test analysis of the frequencies indicated that there is a statistically significant difference between the two groups ($p < 0.01$), whereas there was not a statistically significant difference within the wild-type EVH2 group (Figure 4B). These results demonstrate that in the absence of CP, Ena/VASP proteins robustly promote filopodia. Mutation or deletion of the EVH2 domain interferes with this function despite the presence of endogenous filopodial bundlers such as fascin. This suggests that Ena/VASP proteins must function upstream of filopodial bundling, most likely during the initiation of their formation. Further evidence for this role in filopodia initiation comes from the requirement of all functional domains within the EVH2 domain, including the G-actin–binding site, for robust filopodia formation in our assay. After CP depletion, MV^{D7}-GAB mutant (VASP) exhibited the hyper-ruffling phenotype (~60% of cells, n = 103; Figure 4A). Interestingly, Schirenbeck *et al.* (2006) concluded that bundling by the FAB motif of dVASP alone was required for filopodia formation. Here, we establish that mutations in Ena/VASP, which prevent G-actin binding and tetramerization, also inhibited filopodia formation, demonstrating that filopodia formation requires more than bundling by the FAB motif (Figure 4A). Recently, Co *et al.* (2007) determined that the WH2 domain of N-WASP was the minimal domain needed for barbed end capture, and mutations to this domain ablated the asymmetric distribution at the membrane actin interface inhibiting this activity. The WH2 domain of N-WASP and the GAB motif of Ena/VASP share close homology and could very well function similarly in both proteins. Mutations to the GAB domain may inhibit filopodia formation because of defects in Ena/VASP's ability to capture barbed ends during the initiation of filopodia formation.

Phosphorylation at Key Serine Residues in Mena Promotes Filopodia Formation

Ena/VASP function is regulated by phosphorylation of serine/threonine residues by cAMP/cGMP-dependent PKA and PKG, respectively (Waldmann *et al.*, 1987; Gertler *et al.*, 1996; Lambrechts *et al.*, 2000). In neurite shafts and neurons, the treatment with Netrin-1, a neuronal chemotactic factor, coincided with increased Mena phosphorylation at serine 236 adjacent to the PRO domain, resulting in enhanced filopodia formation (Lebrand *et al.*, 2004). To test whether regulation of Ena/VASP by phosphorylation could also control filopodia formation, we used MV^{D7} cell lines stably expressing phospho-mimetic and nonphosphorylatable mutants of Ena/VASP (Table 1). We first tested the two sites within Mena: the conserved Serine 236 common to all vertebrate Ena/VASP family members and Serine 376 adjacent to the GAB site. Substituting both phosphorylation sites with alanine to mimic the unphosphorylated state (Mena-AA) did not result in efficient induction of filopodia upon CP depletion. Instead the knockdown of CP caused over 70% of transfected cells to show the Ruffling phenotype (Table 1). Conversely, substituting these residues with aspartic acid to mimic the phosphorylated state (Mena-DD) led to filopodia formation in 57% (n = 61) of cells after CP depletion (Table 1), a level equivalent to that of wild-type protein. Accordingly, the distribution of phenotypes in Mena-AA mutant cells, but not Mena-DD cells, was significantly different from cells with wild-type EVH2 domains (Figure 4 and Table 1).

The phosphorylation sites found near the PRO domain and GAB motif of Mena are also conserved in VASP. The equivalent residues in VASP are Serine 153 found in the PRO domain and Serine 235 found adjacent to the GAB motif. However, VASP harbors an additional phosphorylation site, Threonine 274, found adjacent to the FAB motif (Horstrup *et al.*, 1994; Harbeck *et al.*, 2000; Kwiatkowski *et al.*, 2003). CP depletion in cell lines with nonphosphorylatable VASP point mutants, VASP(S153A) (n = 327), VASP(S235A, T274A) (n = 454), and VASP(S153A,S235A,T274A) (n = 232), resulted in both filopodia and ruffle formation at approximately equal frequencies (40–45%; Table 1). Again, we compared these ratios to cell lines with wild-type EVH2 domains by χ^2-test and found a statistically significant difference. When we compared the frequencies of these VASP phosphorylation mutants to the average ratios of the mutant EVH2 group, we also found a statistically significant difference. Under normal spreading conditions, where CP levels were not perturbed, these mutants were similar to other cell lines with a wild-type EVH2 domain. No other cell line demonstrated this behavior. Thus, the VASP phosphorylation mutants, being statistically significantly different form both groups after CP-depletion, comprise a unique group and may explain the mixed phenotype in the assay. These results indicate that the phosphorylation of different residues within VASP may act to fine-tune the function of VASP, leading to more subtle phenotypes.

The EVH2 Domain of VASP But Not Full-Length VASP Bundles Actin In Vivo To Initiate Robust Filopodia Formation

Our experiments demonstrate that the EVH2 domain is essential to filopodia formation in MV^{D7} derivative cell lines. To determine whether the EVH2 domain is also sufficient to

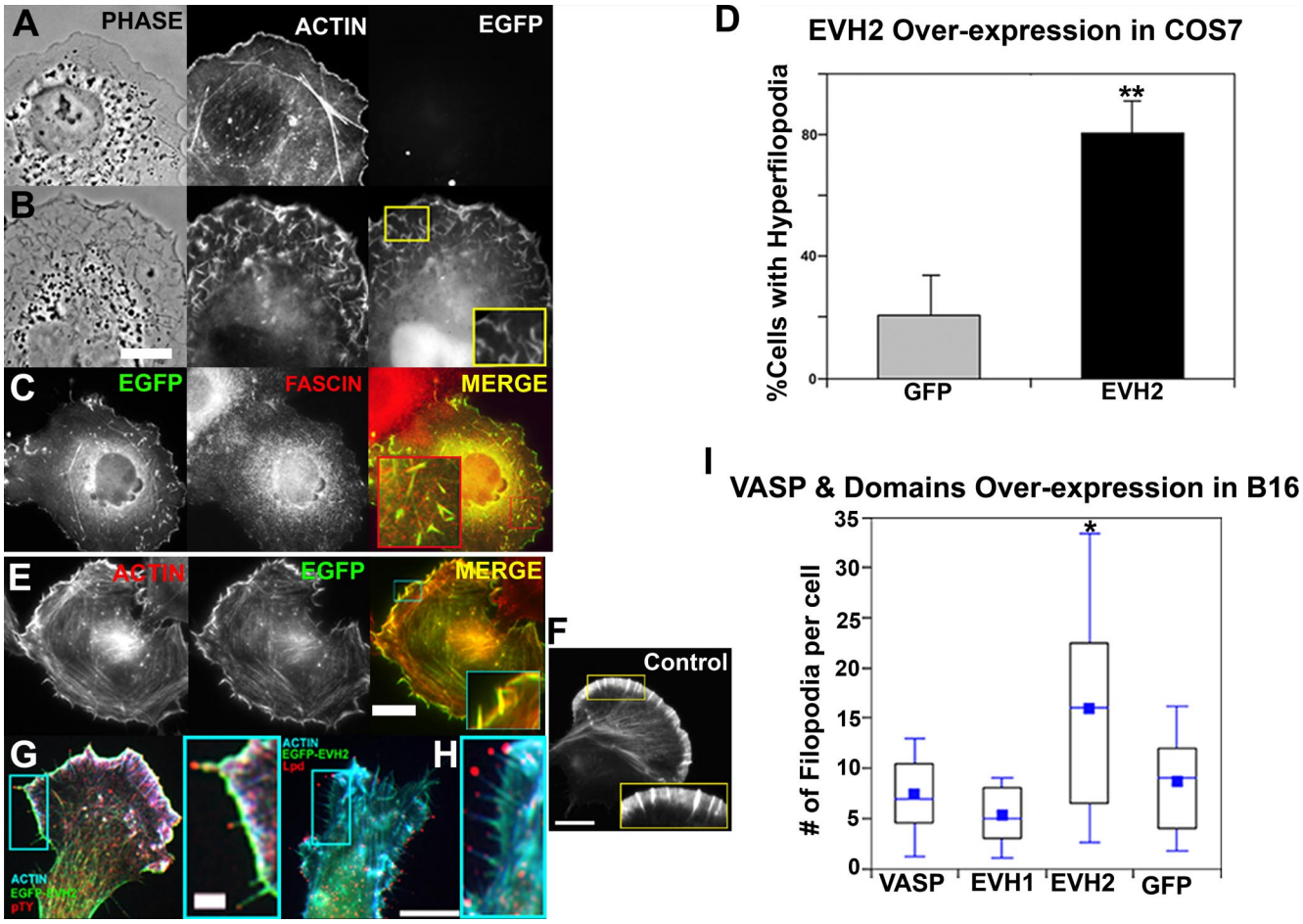

Figure 5. EVH2 domain is sufficient to induce filopodia in other cell lines. (A–D) Induction of filopodia by the EVH2 domain of VASP in COS7 cells. (A and B) F-actin organization of nontransfected (A) and EGFP-EVH2-expressing (B) COS7 cells. Phase-contrast and phalloidin-staining images are shown. Expression of the EVH2 domain induced numerous filopodia. (C) Immunostaining of fascin (middle panel; red in right panel) in COS7 cells overexpressing EGFP-EVH2 (left panel; green in right panel). The inset in right panel shows higher magnification of the boxed region. Fascin and EGFP-EVH2 are colocalized in dorsal filopodia. (D) Quantification of hyper-filopodial phenotype in COS7 cells. Bar graph indicates the percentage of the hyper-filopodial phenotype in cells expressing EGFP-control and EGFP-EVH2 (**$p < 0.02$, Student's t test, $n = 3$). (E–I) Overexpression of the EVH2 domain of VASP induces hyper-filopodial formation in B16F1 mouse melanoma cells. (E) F-actin staining (left panel; red in right panel) and EGFP-EVH2 (middle panel; green in right panel). EGFP-EVH2 localizes along the length of filopodia as well as stress fibers. Boxed region shows, at higher magnification, colocalization of EVH2 domain and actin. Scale bar, 10 μm. (F) Actin by phalloidin staining of a nontransfected control B16F1 displaying typical filopodial amounts and distributions. (G and H) Localization of the filopodial tip markers in EVH2-induced filopodia. B16F1 cell expressing EGFP-EVH2 (green), immunostained with anti-phospho-tyrosine (G, red) or anti-lamellipodin (H, red). F-actin (blue) was visualized by phalloidin staining. Scale bar, 10 μm. Boxed region is higher magnification of EVH2 induced filopodia. Scale bar, 2 μm. Both molecular markers were concentrated at the filopodia tips. (I) Box-and-whisker plot comparing the number of filopodia per B16F1 cell transiently expressing full-length VASP, EVH1 domain of VASP, EVH2 domain of VASP, and EGFP-control. The small square indicates the mean, the line in the middle of the box the median. The top of the box indicates the third quartile, the bottom of the both the first quartile. The upper and lower boundary of each whisker represents 90th and 10th percentile of the data respectively (*$p < 0.02$, one-way ANOVA).

induce filopodia in other cell lines, we transiently expressed EGFP-EVH2 (VASP) in COS7 cell lines. COS7 cells, when plated on fibronectin, rarely form filopodia under normal cell culture conditions (Bohil *et al.*, 2006; Loitto *et al.*, 2007). This system was, therefore, ideal for testing the ability of EGFP-EVH2 to induce filopodia (Figure 5A). On expression of EGFP-EVH2, over 80% ($n = 201$) of transfected COS7 cells formed filopodia-like protrusions at the cell periphery, which was visible by both phase-contrast microscopy and fluorescent microscopy when stained for phalloidin (Figure 5B). These protrusions were also visible on the dorsal surface (Figure 5B, inset). Although COS7 cells are a fibroblastic cell line that usually do not form microvilli, we confirmed that these protrusions were genuine filopodia by immunostaining for fascin, a predominately filopodial bundler (Adams and Schwartz, 2000; Bartles, 2000; Loomis *et al.*, 2003; Tilney *et al.*, 2004; Vignjevic *et al.*, 2006). Both the EVH2 domain of VASP and fascin localize to these dorsal filopodia (Figure 5C). Approximately 20% of COS7 cells expressing the EGFP-control vector showed this hyper-filopodial phenotype. These results demonstrate that the potential of the Ena/VASP EVH2 domain to induce filopodia is not only limited to MV^{D7} cells.

Overexpression of the EVH2 domain in COS7 fibroblasts indicates that the EVH2 domain is a potent initiator of filopodia, mostly through its actin filament barbed end cross-linking activity. Similarly, Schirenbeck *et al.* (2006) found that dVASP bundles actin in vivo and that this bun-

dling activity is required for filopodia formation in *Dictyostelium*. However, when we overexpressed VASP in B16F1 mouse melanoma cells (n = 20), a cell line that generally forms both lamellipodia and filopodia under normal cell culturing conditions (Figure 5F), we did not find a statistically significant increase in the number of filopodia per cell over cells expressing an EGFP-control vector (n = 20; Figure 5I). Only when we overexpressed EVH2 domain of VASP (n = 20) did we observe a statistically significant increase in the number of filopodia per cell (Figure 5, D and H). We immunostained these filopodia for two characteristic filopodial tip markers, lamellipodin, and phospho-tyrosine (Figure 5, G and H). Both lamellipodin and phospho-tyrosine localized to the tips of EVH2-induced filopodia, similar to their distributions in filopodia formed in the other cell types (unpublished data; Krause *et al.*, 2004). This effect was specific to the EVH2 domain because overexpression of the EVH1 domain of VASP did not lead to an increase in filopodia. These results suggest that although Ena/VASP proteins may be potent bundlers of actin filaments in vitro via the EVH2 domain, it is not likely their physiological role because overexpression of full-length VASP fails to significantly increase the number of filopodia in cells.

VASP Exchanges Rapidly at the Leading Edge of Lamellipodia But Very Slowly at Filopodial Tips

The Ena/VASP family of proteins localizes to both the leading edge of lamellipodia and filopodial tips where they function to regulate actin dynamics. Productive lamellipodial protrusion requires a defined length of actin filaments. To prevent overelongation of actin filaments in lamellipodia, the association between VASP and barbed ends must be transient in vivo. In contrast, if the role of Ena/VASP proteins is to cross-link actin barbed ends and prevent premature filament termination, as predict, then the association between VASP and barbed ends in filopodial tips would be relatively stable.

To test these concepts, we used FRAP to measure the recovery dynamics of full-length VASP, EVH1, or EVH2 domain of VASP, at filopodial tips and the leading edge of protruding lamellipodia. We used B16F1 cells that transiently expressed EGFP-tagged VASP or the EVH1 domain of VASP because these cells readily from both lamellipodia and filopodia and are easily transfectable, making them amenable to imaging. This was important because our FRAP system utilizes a laser scanning confocal microscope, and exogenous expression of EGFP-VASP in B16 was brighter than EGFP-tagged Ena/VASP proteins stably integrated in MV^{D7} cells because their expression levels were carefully selected by FAC sorting (Geese *et al.*, 2002; Loureiro *et al.*, 2002). In addition, we used MV^{D7} cells expressing EGFP-EVH2 to prevent tetramerization with endogenous Ena/VASP proteins. The results of the FRAP analysis of full-length EGFP-VASP in B16F1 cells yielded different half-times of recovery in lamellipodia and filopodia. In filopodial tips we observed virtually no recovery of fluorescence (n = 15; Figure 6A). We also bleached both protruding as well as stable filopodia, which did not reveal significant fluorescent

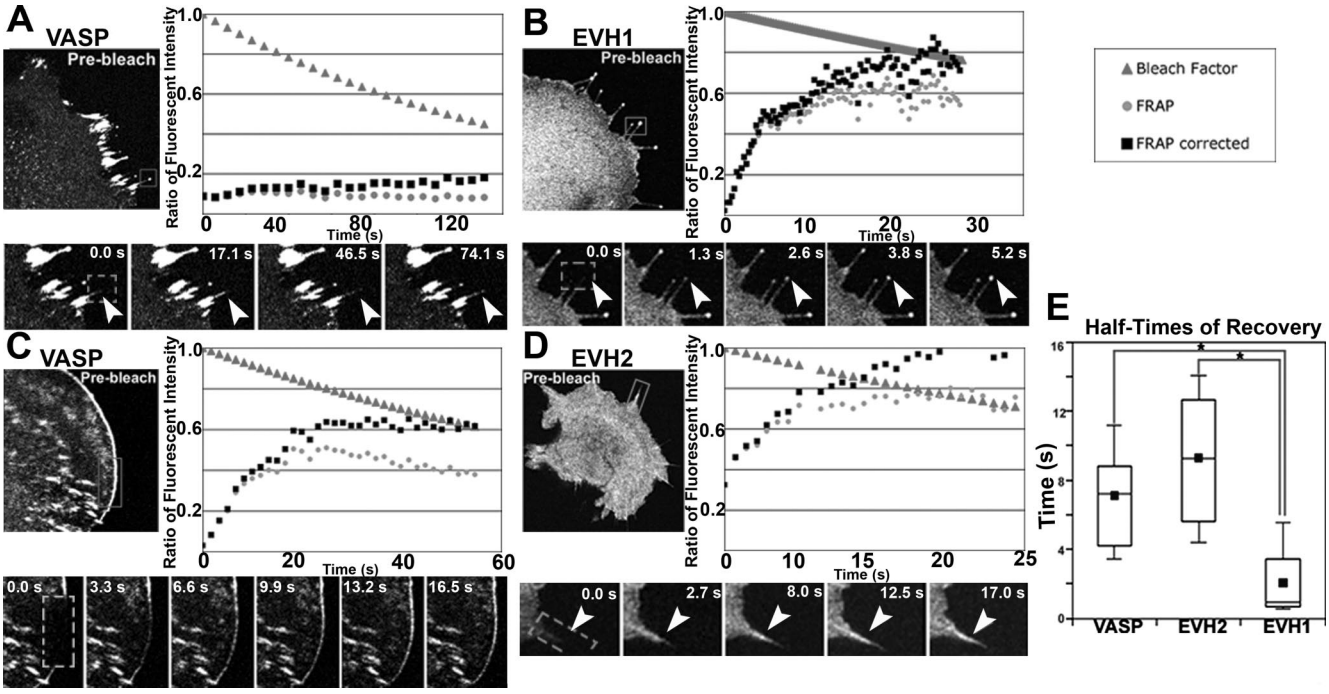

Figure 6. Fluorescent recovery after photobleaching (FRAP) of VASP, EVH1, and EVH2 Domain of VASP. (A–D) Graphs are representative of FRAP data of the full-length VASP (A and C), the EVH1 domain (B), and the EVH2 domain (D). FRAP analysis are shown for filopodia (A, B, and D) and lamellipodia (C). In lower magnification images (top left) show the prebleach images. The regions indicated by gray rectangles are shown in the time series of fluorescence recovery (bottom). The white arrowheads indicate either filopodial tips (A and B) or shaft (D). Gray boxes denote the bleached regions subject to quantification. The fluorescence recovery for each sample was presented as a graph (top right). The gray triangles represent theoretical values of decrease in fluorescence intensity due to laser illumination during image acquisition. The gray circles represent fluorescent intensity normalized to the pre-bleached images. The black squares represent the relative intensity after correction for photofading during image acquisition. Time is given in seconds. (E) Box-and-whisker plot of the distribution of the half recovery times of FRAP analysis in the leading edges of lamellipodia (VASP), leading edge and filopodial shafts (EVH2), and filopodial tips (EVH1; *$p < 0.001$, Student's *t* test).

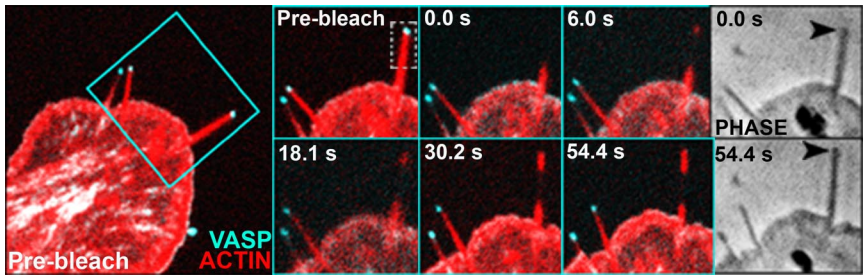

Figure 7. Co-FRAP of EGFP-VASP and mCherry-Actin. Sequential photobleaching of EGFP-VASP (cyan) and mCherry-Actin (red) of a protruding filopodium. Lower magnification image shows prebleach fluorescence image, with a cyan box representing the region of higher magnification. In higher magnification, time-lapsed fluorescence images are shown with the bleached region indicated by gray box. Two phase-contrast images at the beginning (top) and end (bottom) of time sequence, with black arrows denoting the tip of bleached filopodium. Note that the filopodium continued protrusion during the course of time-lapsed imaging.

recovery. This same trend was found in cells expressing EGFP-Mena (unpublished data). An initial concern regarding the lack of fluorescence recovery of VASP at filopodial tips was that the narrow structure of filopodia might represent a barrier to diffusion. Because the EVH1 domain of VASP readily localized to filopodial tips, we extended our FRAP analysis to this domain (Figure 6B). The recovery of the EVH1 domain was extremely rapid, $t_{1/2} = 3.3 \pm 4.7$ s ($n = 15$). This result demonstrates that the lack of recovery we observed with full-length VASP at filopodial tips was not a result of limited diffusion within the structure.

In contrast to filopodial tips, fluorescent recovery of VASP at the leading edge of lamellipodia showed rapid dynamics with a half time of recovery of 8.4 ± 5.3 s ($n = 15$; Figure 6C). Similarly, we found the recovery of the EVH2 domain within filopodial shafts to be 13.7 ± 10.3 s ($n = 10$; Figure 6D). The fluorescence recovery of VASP at the leading edge and at EVH2 domain along filopodial shafts was statistically indistinguishable (Figure 6E). Similar results were obtained for EGFP-Mena at the leading edge (unpublished data). Although the fluorescence recovery of VASP and the EVH2 domain represent unbinding and binding events during lamellipodial protrusion, the recovery of EVH1 could be the result of the same kinetics but at a faster time scale, associating with and dissociating from a membrane-bound ligand. These findings also suggest that VASP transitions from a more dynamic association at the leading edge of the lamellipodium to one that is more static as filopodia form from the lamellipodium cytoskeleton. This result supports the proposed "processive step" model where Ena/VASP molecules retain tip localization despite continuous insertional polymerization at the barbed end (Chereau and Dominguez, 2006).

To further investigate this concept we coexpressed mCherry-actin and EGFP-VASP in B16F1 cells and sequentially photobleached both tagged molecules at the distal end of a protruding filopodium (Figure 7A). B16F1 cells show a considerably higher transfection efficiency than MV^{D7} derivative cells, which made using them much more convenient for this study. Again, we observed a lack of fluorescent recovery by EGFP-VASP at the filopodial tip despite continued filopodial protrusion; however, we did observe fluorescent recovery of mCherry-actin. The mCherry-actin first appeared at the distal portion of the filopodia and underwent retrograde flow within the filopodium as it the filopodium continued to protrude. This result demonstrates that at the resolution of the light microscope, Ena/VASP allows for insertional polymerization of actin while maintaining filopodial tip localization. In summary, Ena/VASP proteins transition from a lamellipodial to filopodial localization, and in doing so, undergoes a change in kinetics, that is, once filopodia formation is initiated, Ena/VASP proteins transition to a more "static" association with actin filaments. In addition Ena/VASP facilitates insertional polymerization of actin at filopodial tips. Collectively, these results illustrate how Ena/VASP functions as a barbed end cross-linker that facilitates the transition from a lamellipodial to a filopodial mode of protrusion.

The G-actin–binding Domain Is Needed to Maintain Distal Tip Positioning During Filopodial Protrusion

Results from the FRAP analysis presented here indicate that Ena/VASP proteins maintain their distal positioning during filopodial protrusion. Next, we determined which domains within Ena/VASP are critical for this localization and subsequent activities. We used the MV^{D7} derivative cell lines in combination with FRAP to photobleach protruding filopodial tips. We limited the analysis to those cell lines that showed specific filopodial tip localization, namely MV^{D7}-VASP, MV^{D7}-ΔFAB (VASP), MV^{D7}-GAB mutant (VASP), MV^{D7}-ΔPRO (Mena), MV^{D7}-AA (Mena), and MV^{D7}-DD (Mena) (Supplementary Figure 1). We imaged the filopodial tips of fully spread cells by phase-contrast microscopy as well as by confocal fluorescence microscopy to track the dynamics of Ena/VASP domains in filopodia. As observed previously, we did not see fluorescent recovery in cell lines expressing full-length VASP at filopodial tips over the time course of the experiment (Figure 8A, Supplementary Figure 2A). We observed this same trend in filopodia from MV^{D7}-ΔPRO (Mena), MV^{D7}-AA (Mena), and MV^{D7}-DD (Mena) cell lines (data not shown). However, after photobleaching of filopodial tips in the MV^{D7}-GAB mutant (VASP) cell line, we observed a slow protracted fluorescent recovery in over half the protruding filopodia ($n = 26$; Figure 8B). These protruding filopodial tips collectively had an average half time of recovery of 40 s, recovering to 35–50% of the fluorescent intensity (Supplementary Figure 2, B, D, and E). We did not observe this behavior in filopodial tips from MV^{D7}-ΔFAB (VASP) cells, where 99% of protruding filopodia ($n = 20$) did not exhibit fluorescent recovery, demonstrating that this behavior is specific to the G-actin–binding mutant (Figure 8C, Supplementary Figure 2, C–E). These results indicate that the G-actin–binding motif of Ena/VASP proteins plays a key role in maintaining filopodial tip localization during protrusion and likely collaborates with the N-terminal EVH1 domain in positioning the full-length protein. Additionally, these results support the recent findings of Co *et al.* (2007) regarding barbed end capture by the WH2 domain of N-WASP. Mutations to the GAB motif in VASP may also inhibit barbed end capture, leading to more frequent dissociation of this mutant from filopodial tips.

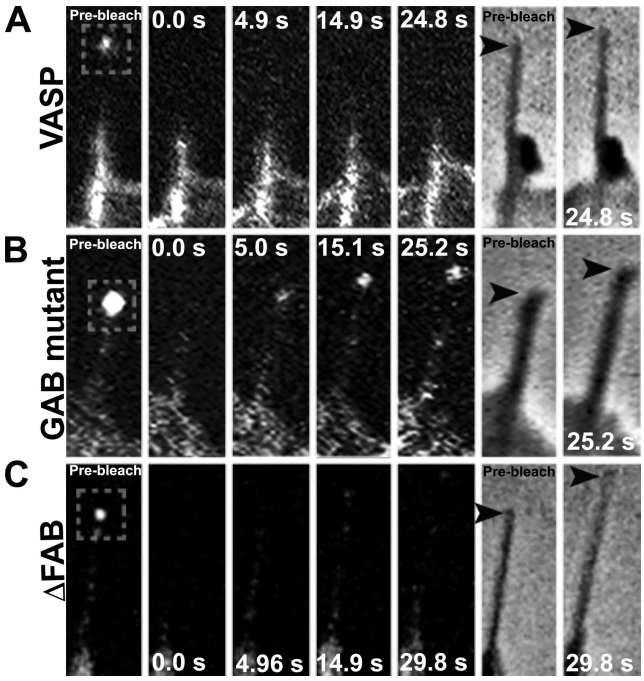

Figure 8. FRAP of filopodial tips in MV^{D7}-derivative stable cell lines. Time-lapsed fluorescence and phase-contrast images of photobleached filopodial tips in MV^{D7} derivative cell lines. (A) MV^{D7}-VASP, (B) MV^{D7}-GAB mutant (VASP), and (C) MV^{D7}-ΔFAB(VASP). The first image of the fluorescence sequence shows the prebleached filopodium with gray boxes indicating the regions of quantification in Supplementary Figure 2. Phase-contrast images are shown at the prebleach and the final time points. Black arrows, which denote filopodial tips, demonstrate filopodia protrusion during image acquisition.

DISCUSSION

Ena/VASP proteins are comprised of two modules, a membrane-targeting module and an actin-interacting module (Figure 9A). The membrane-targeting module is composed of a membrane-bound ligand and the EVH1 domain that binds this ligand. Deletion of the EVH1 domain ablates filopodial tip localization and leads to a broader lamellipodial distribution as opposed to the specific leading edge localization, characteristic of full-length Ena/VASP. The actin-interacting module is composed of the EVH2 domain including the GAB, FAB, and COCO motifs. The EVH2 domain is the minimal domain required for filopodia formation. We suggest the following model for Ena/VASP-initiated filopodia formation: Ena/VASP is recruited to the leading edge by binding to membrane-bound ligands via the EVH1 domain (Figure 9B, 1). This interaction is transient, and associations with actin filaments are required to stabilize the full-length molecule at filopodial tips. It is likely that stabilization is dependent on a complex formed between the GAB motif and actin filament barbed ends (Figure 9B, 2). To allow for continuous polymerization by insertion of G-actin, this interaction is transient (Figure 9B, 3). We predict that Ena/VASP initiates filopodia formation through multiple subcellular events. First, they function to cross-link actin barbed ends via tetramerization and simultaneous interaction with actin filaments. Concomitantly, they undergo a change in kinetics that supports filopodial tip stabilization after a transition from lamellipodial to filopodial localization. Finally, through transient interactions with membrane bound ligands and actin filaments, Ena/VASP maintains tip localization and enhances continued actin polymerization.

The EVH2 domain has been previously shown to be the minimally functioning unit of Ena/VASP in whole cell motility and anti-capping (Bear *et al.*, 2000; Loureiro *et al.*, 2002; Barzik *et al.*, 2005). Deletion or mutation of the GAB or FAB motifs or the COCO domain ablates Ena/VASP anti-capping (Barzik *et al.*, 2005). Similarly, in this study, we found that EVH2 is the minimal functional unit for filopodia formation and all three motifs, GAB, FAB, and COCO, are necessary for filopodia formation. Given that the initiation of filopodia formation requires the antagonism of filament termination and that filopodia seem to be an important component of cell motility, our data may provide a mechanistic link between the earlier findings. We have determined that the EVH2 domain has a role that goes beyond anticapping activity in filopodia formation; mutations/deletions to the domain, even in absence of CP, inhibits filopodia formation. Given the importance of the EVH2 domain to filopodia formation in fibroblasts, it is interesting to note the EVH2 domain of Ena/VASP proteins is not sufficient for filopodia formation in neurons (Dent and Gertler, unpublished data).

Schirenbeck *et al.* (2006) hypothesized that the bundling activity of the FAB motif in dVASP was required for filopodia formation . Our data suggest that in addition to the bundling function of the FAB site, the GAB motif is required. Moreover, the FAB motif of Ena/VASP has been shown to be important for localization of Ena/VASP to actin bundles, anticapping, and the incorporation of G-actin into filaments (Bachmann *et al.*, 1999; Bear *et al.*, 2002; Loureiro *et al.*, 2002;

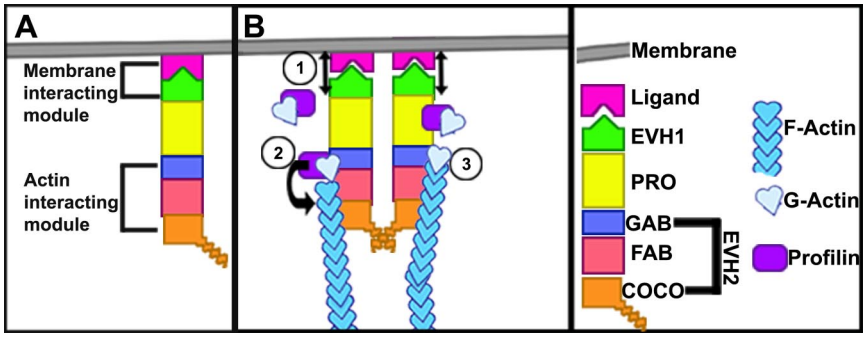

Figure 9. Model of Ena/VASP-initiated filopodia formation. (A) Ena/VASP molecules can be divided into two modules: membrane-interacting module and actin-interacting module. (B, 1–3) Initiation of filopodia by Ena/VASP proteins. (B, 1) Ena/VASP is recruited to membrane ligands via a transient association with the EVH1 domain. (B, 2) Additional interactions with the G-actin– and F-actin–binding domain help to stabilize molecule at filopodial tips. (B, 3) The complex formed between the G-actin–binding domain of Ena/VASP, the actin barbed end and G-actin is also somewhat transient in nature to allow for insertional polymerization. Collectively the interaction between the EVH1 domain and the membrane-bound ligand, the G-actin–binding domain, and the actin barbed end, and tetramerization of the coiled-coil domain allows for the entire molecule to be "static" and filopodial tips, but flexible enough to for continued insertional actin polymerization.

Barzik *et al.*, 2005). Analysis of a mutant VASP protein harboring a deletion of the F-acting–binding motif does not distinguish between these different functions. Additionally, there are major differences between dVASP and the mammalian counterparts, including the lack of serine/threonine phosphorylation sites (Schirenbeck *et al.*, 2006).

Structural and biochemical work from Chereau and Dominguez (2006) indicates that the GAB motif has a higher affinity for profilin-actin then for G-actin, which led the authors to propose a model whereby the PRO domain adjacent to the GAB motif cooperates in the "priming" of profilin-actin to the barbed end of filaments, which leads to a processive stepwise mechanism to explain the association of Ena/VASP with the barbed ends during filament elongation. Barzik *et al.* (2005) also hypothesize that Ena/VASP maintains their barbed end localization while simultaneously preventing filament termination, promoting filament elongation. Results from our FRAP analysis of Ena/VASP at filopodial tips lends support to these models. We did not observe fluorescent recovery of VASP at filopodial tips, indicating a lack of exchange of molecules even as filopodia continue to grow. When we bleached filopodial tips in the cell line harboring mutations in the GAB motif, we observed limited fluorescent recovery, suggesting that the GAB motif plays an integral role in the maintenance of filopodial tip localization and further supports models proposed by Chereau and Dominguez, Barzik, and others. In addition, we directly observed the fluorescent recovery of mCherry-actin at the distal tip of filopodia despite the lack of recovery of EGFP-VASP, indicating that at the level of the light microscope, Ena/VASP allows for insertional polymerization of actin. A similar processive stepwise model has also been proposed to explain how the formin family of molecules maintains their association with actin filaments but allows for continued actin polymerization (Zigmond *et al.*, 2003).

Co *et al.* (2007) demonstrated that the WH2 domain of N-WASP, which shares homology to the GAB motifs in Ena/VASP, is essential to barbed end capture. Although the concept of membrane anchoring is not new (Laurent *et al.*, 1999; Samarin *et al.*, 2003), this is first time it has been narrowed to this domain. Similar mutations that inhibited barbed end capture by the WH2 domain were made to the GAB motif and tested here. It is likely that the deficiencies we found in filopodia formation and stabilization of the GAB mutant at filopodial tips is a result of the similar inhibition of barbed end capture and implicates a possible role of barbed end capture by the GAB motif of Ena/VASP.

Both formins and Ena/VASP are part of the filopodial tip complex (Reinhard *et al.*, 1992; Lanier *et al.*, 1999; Rottner *et al.*, 1999; Pellegrin and Mellor, 2005). It has been hypothesized that formins and VASP cooperate during filopodia formation (Schirenbeck *et al.*, 2005). Unlike the *Dictyostelium* dDia2 and dVASP, the mammalian counterparts induce filopodia independently of each other (Barzik and Gertler, unpublished data). This can probably be explained by the structural differences between dVASP and the mammalian Ena/VASP proteins.

Phosphorylation of Mena in neurons has a positive effect on filopodia formation (Lebrand *et al.*, 2004). Results from our filopodia formation assay conclude that phosphorylation positively regulates filopodia formation by Mena, however, we found that phosphorylation of VASP had a more intermediate phenotype. Phosphorylation of Ena/VASP had differential effects in anticapping (Loureiro *et al.*, 2002; Barzik *et al.*, 2005) and bundling (Harbeck *et al.*, 2000; Barzik *et al.*, 2005), depending on which residue is phosphorylated. Howe *et al.* (2002) demonstrated that VASP undergoes cycles of global phosphorylation and dephosphorylation as cells adhere and spread. It has yet to be determined whether these cyclic phosphorylation events affect the total cellular pool or only bound VASP. It is not clear from this study if Mena cycles through similar phosphorylation-dephosphorylation states. VASP is distinguished from Mena by an additional PKA/PKG site, Threonine 274, which might be required for fine-tuning of VASP during special activities. Our data from the CP-depletion assay suggests that filopodia formation could be such an activity during which VASP and Mena might be regulated differently by phosphorylation.

ACKNOWLEDGMENTS

We thank Drs. Edwin Taylor, Sarah Rice, and Omar Quintero for critical reading of the manuscript and Dr. Teng-Leong Chew and Yvonne Aratyn for assistance with the photobleaching experiments. This work was supported in part by National Institutes of Health Grants GM7542201 to D.A.A., GM58801 to F.B.G., and GM62431 to G.G.B. and by Cell Migration Consortium Grants GM64346 to D.A.A and G.G.B.

REFERENCES

Adams, J. C., and Schwartz, M. A. (2000). Stimulation of fascin spikes by thrombospondin-1 is mediated by the GTPases Rac and Cdc42. J. Cell Biol. *150*, 807–822.

Ahern-Djamali, S. M., Bachmann, C., Hua, P., Reddy, S. K., Kastenmeier, A. S., Walter, U., and Hoffmann, F. M. (1999). Identification of profilin and src homology 3 domains as binding partners for *Drosophila* enabled. Proc. Natl. Acad. Sci. USA *96*, 4977–4982.

Albrecht-Buehler, G. (1976). Filopodia of spreading 3T3 cells. Do they have a substrate-exploring function? J. Cell Biol. *69*, 275–286.

Bachmann, C., Fischer, L., Walter, U., and Reinhard, M. (1999). The EVH2 domain of the vasodilator-stimulated phosphoprotein mediates tetramerization, F-actin binding, and actin bundle formation. J. Biol. Chem. *274*, 23549–23557.

Ballestrem, C., Wehrle-Haller, B., and Imhof, B. A. (1998). Actin dynamics in living mammalian cells. J. Cell. Sci. *111 (Pt 12)*, 1649–1658.

Bartles, J. R. (2000). Parallel actin bundles and their multiple actin-bundling proteins. Curr. Opin. Cell Biol. *12*, 72–78.

Barzik, M., Kotova, T. I., Higgs, H. N., Hazelwood, L., Hanein, D., Gertler, F. B., and Schafer, D. A. (2005). Ena/VASP proteins enhance actin polymerization in the presence of barbed end capping proteins. J. Biol. Chem. 280, 28653–28662.

Bear, J. E., Loureiro, J. J., Libova, I., Fassler, R., Wehland, J., and Gertler, F. B. (2000). Negative regulation of fibroblast motility by Ena/VASP proteins. Cell *101*, 717–728.

Bear, J. E. *et al.* (2002). Antagonism between Ena/VASP proteins and actin filament capping regulates fibroblast motility. Cell *109*, 509–521.

Bearer, E. L., Prakash, J. M., Manchester, R. D., and Allen, P. G. (2000). VASP protects actin filaments from gelsolin: an in vitro study with implications for platelet actin reorganizations. Cell Motil. Cytoskelet. *47*, 351–364.

Bohil, A. B., Robertson, B. W., and Cheney, R. E. (2006). Myosin-X is a molecular motor that functions in filopodia formation. Proc. Natl. Acad. Sci. USA *103*, 12411–12416.

Carl, U. D., Pollmann, M., Orr, E., Gertlere, F. B., Chakraborty, T., and Wehland, J. (1999). Aromatic and basic residues within the EVH1 domain of VASP specify its interaction with proline-rich ligands. Curr. Biol. *9*, 715–718.

Chakraborty, T. *et al.* (1995). A focal adhesion factor directly linking intracellularly motile *Listeria monocytogenes* and *Listeria ivanovii* to the actin-based cytoskeleton of mammalian cells. EMBO J. *14*, 1314–1321.

Chereau, D., and Dominguez, R. (2006). Understanding the role of the G-actin-binding domain of Ena/VASP in actin assembly. J. Struct. Biol. *155*, 195–201.

Co, C., Wong, D. T., Gierke, S., Chang, V., and Taunton, J. (2007). Mechanism of actin network attachment to moving membranes: barbed end capture by N-WASP WH2 domains. Cell *128*, 901–913.

Dent, E. W., and Gertler, F. B. (2003). Cytoskeletal dynamics and transport in growth cone motility and axon guidance. Neuron *40*, 209–227.

Dubin-Thaler, B. J., Giannone, G., Dobereiner, H. G., and Sheetz, M. P. (2004). Nanometer analysis of cell spreading on matrix-coated surfaces reveals two distinct cell states and STEPs. Biophys. J. *86*, 1794–1806.

Ermekova, K. S., Zambrano, N., Linn, H., Minopoli, G., Gertler, F., Russo, T., and Sudol, M. (1997). The WW domain of neural protein FE65 interacts with proline-rich motifs in Mena, the mammalian homolog of *Drosophila* enabled. J. Biol. Chem. *272*, 32869–32877.

Evangelista, M., Zigmond, S., and Boone, C. (2003). Formins: signaling effectors for assembly and polarization of actin filaments. J. Cell Sci. *116*, 2603–2611.

Fedorov, A. A., Fedorov, E., Gertler, F., and Almo, S. C. (1999). Structure of EVH1, a novel proline-rich ligand-binding module involved in cytoskeletal dynamics and neural function. Nat. Struct. Biol. *6*, 661–665.

Geese, M., Loureiro, J. J., Bear, J. E., Wehland, J., Gertler, F. B., and Sechi, A. S. (2002). Contribution of Ena/VASP proteins to intracellular motility of listeria requires phosphorylation and proline-rich core but not F-actin binding or multimerization. Mol. Biol. Cell *13*, 2383–2396.

Gertler, F. B., Comer, A. R., Juang, J. L., Ahern, S. M., Clark, M. J., Liebl, E. C., and Hoffmann, F. M. (1995). enabled, a dosage-sensitive suppressor of mutations in the *Drosophila* Abl tyrosine kinase, encodes an Abl substrate with SH3 domain-binding properties. Genes Dev. *9*, 521–533.

Gertler, F. B., Niebuhr, K., Reinhard, M., Wehland, J., and Soriano, P. (1996). Mena, a relative of VASP and *Drosophila* Enabled, is implicated in the control of microfilament dynamics. Cell *87*, 227–239.

Han, Y. H., Chung, C. Y., Wessels, D., Stephens, S., Titus, M. A., Soll, D. R., and Firtel, R. A. (2002). Requirement of a vasodilator-stimulated phosphoprotein family member for cell adhesion, the formation of filopodia, and chemotaxis in dictyostelium. J. Biol. Chem. *277*, 49877–49887.

Harbeck, B., Huttelmaier, S., Schluter, K., Jockusch, B. M., and Illenberger, S. (2000). Phosphorylation of the vasodilator-stimulated phosphoprotein regulates its interaction with actin. J. Biol. Chem. *275*, 30817–30825.

Hashimoto, Y., Skacel, M., and Adams, J. C. (2005). Roles of fascin in human carcinoma motility and signaling: prospects for a novel biomarker? Int. J. Biochem. Cell Biol. *37*, 1787–1804.

Haviv, L., Brill-Karniely, Y., Mahaffy, R., Backouche, F., Ben-Shaul, A., Pollard, T. D., and Bernheim-Groswasser, A. (2006). Reconstitution of the transition from lamellipodium to filopodium in a membrane-free system. Proc. Natl. Acad. Sci. USA *103*, 4906–4911.

Horstrup, K., Jablonka, B., Honig-Liedl, P., Just, M., Kochsiek, K., and Walter, U. (1994). Phosphorylation of focal adhesion vasodilator-stimulated phosphoprotein at Ser157 in intact human platelets correlates with fibrinogen receptor inhibition. Eur. J. Biochem. *225*, 21–27.

Howe, A. K., Hogan, B. P., and Juliano, R. L. (2002). Regulation of vasodilator-stimulated phosphoprotein phosphorylation and interaction with Abl by protein kinase A and cell adhesion. J. Biol. Chem. *277*, 38121–38126.

Huttelmaier, S., Harbeck, B., Steffens, O., Messerschmidt, T., Illenberger, S., and Jockusch, B. M. (1999). Characterization of the actin binding properties of the vasodilator-stimulated phosphoprotein VASP. FEBS Lett. *451*, 68–74.

Jacinto, A., Martinez-Arias, A., and Martin, P. (2001). Mechanisms of epithelial fusion and repair. Nat. Cell Biol. *3*, E117–E123.

Jacinto, A., Wood, W., Balayo, T., Turmaine, M., Martinez-Arias, A., and Martin, P. (2000). Dynamic actin-based epithelial adhesion and cell matching during *Drosophila* dorsal closure. Curr. Biol. *10*, 1420–1426.

Kojima, S., Vignjevic, D., Borisy, G. G. (2004). Improved silencing vector co-expressing GFP and small hairpin RNA. Biotechniques *36*, 74–79.

Kovar, D. R. (2006). Molecular details of formin-mediated actin assembly. Curr. Opin. Cell Biol. *18*, 11–17.

Krause, M., Dent, E. W., Bear, J. E., Loureiro, J. J., and Gertler, F. B. (2003). Ena/VASP proteins: regulators of the actin cytoskeleton and cell migration. Annu. Rev. Cell Dev. Biol. *19*, 541–564.

Krause, M. *et al.* (2004). Lamellipodin, an Ena/VASP ligand, is implicated in the regulation of lamellipodial dynamics. Dev. Cell *7*, 571–583.

Kuhnel, K., Jarchau, T., Wolf, E., Schlichting, I., Walter, U., Wittinghofer, A., and Strelkov, S. V. (2004). The VASP tetramerization domain is a right-handed coiled coil based on a 15-residue repeat. Proc. Natl. Acad. Sci. USA *101*, 17027–17032.

Kwiatkowski, A. V., Gertler, F. B., and Loureiro, J. J. (2003). Function and regulation of Ena/VASP proteins. Trends Cell Biol. *13*, 386–392.

Lambrechts, A., Kwiatkowski, A. V., Lanier, L. M., Bear, J. E., Vandekerckhove, J., Ampe, C., and Gertler, F. B. (2000). cAMP-dependent protein kinase phosphorylation of EVL, a Mena/VASP relative, regulates its interaction with actin and SH3 domains. J. Biol. Chem. *275*, 36143–36151.

Lanier, L. M., Gates, M. A., Witke, W., Menzies, A. S., Wehman, A. M., Macklis, J. D., Kwiatkowski, D., Soriano, P., and Gertler, F. B. (1999). Mena is required for neurulation and commissure formation. Neuron *22*, 313–325.

Laurent, V., Loisel, T. P., Harbeck, B., Wehman, A., Grobe, L., Jockusch, B. M., Wehland, J., Gertler, F. B., and Carlier, M. F. (1999). Role of proteins of the Ena/VASP family in actin-based motility of *Listeria monocytogenes*. J. Cell Biol. *144*, 1245–1258.

Lebrand, C., Dent, E. W., Strasser, G. A., Lanier, L. M., Krause, M., Svitkina, T. M., Borisy, G. G., and Gertler, F. B. (2004). Critical role of Ena/VASP proteins for filopodia formation in neurons and in function downstream of netrin-1. Neuron *42*, 37–49.

Loitto, V. M., Huang, C., Sigal, Y. J., and Jacobson, K. (2007). Filopodia are induced by aquaporin-9 expression. Exp. Cell Res. *313*, 1295–1306.

Loomis, P. A., Zheng, L., Sekerkova, G., Changyaleket, B., Mugnaini, E., and Bartles, J. R. (2003). Espin cross-links cause the elongation of microvillus-type parallel actin bundles in vivo. J. Cell Biol. *163*, 1045–1055.

Loureiro, J. J., Rubinson, D. A., Bear, J. E., Baltus, G. A., Kwiatkowski, A. V., and Gertler, F. B. (2002). Critical roles of phosphorylation and actin binding motifs, but not the central proline-rich region, for Ena/vasodilator-stimulated phosphoprotein (VASP) function during cell migration. Mol. Biol. Cell *13*, 2533–2546.

Mejillano, M. R., Kojima, S., Applewhite, D. A., Gertler, F. B., Svitkina, T. M., and Borisy, G. G. (2004). Lamellipodial versus filopodial mode of the actin nanomachinery: pivotal role of the filament barbed end. Cell *118*, 363–373.

Mitchison, T. J., and Cramer, L. P. (1996). Actin-based cell motility and cell locomotion. Cell *84*, 371–379.

Mogilner, A., and Edelstein-Keshet, L. (2002). Regulation of actin dynamics in rapidly moving cells: a quantitative analysis. Biophys. J. *83*, 1237–1258.

Mogilner, A., and Rubinstein, B. (2005). The physics of filopodial protrusion. Biophys. J. *89*, 782–795.

Niebuhr, K., Ebel, F., Frank, R., Reinhard, M., Domann, E., Carl, U. D., Walter, U., Gertler, F. B., Wehland, J., and Chakraborty, T. (1997). A novel proline-rich motif present in ActA of *Listeria monocytogenes* and cytoskeletal proteins is the ligand for the EVH1 domain, a protein module present in the Ena/VASP family. EMBO J. *16*, 5433–5444.

Pellegrin, S., and Mellor, H. (2005). The Rho family GTPase Rif induces filopodia through mDia2. Curr. Biol. *15*, 129–133.

Pollard, T. D., Blanchoin, L., and Mullins, R. D. (2000). Molecular mechanisms controlling actin filament dynamics in nonmuscle cells. Annu. Rev. Biophys. Biomol. Struct. *29*, 545–576.

Pollard, T. D., and Borisy, G. G. (2003). Cellular motility driven by assembly and disassembly of actin filaments. Cell *112*, 453–465.

Porter, K. R., Cluade, A., and Fullam, E. F. (1945). A study of tissue culture cells by electron microscopy. J. Exp. Med. *81*, 233–246.

Reinhard, M., Halbrugge, M., Scheer, U., Wiegand, C., Jockusch, B. M., and Walter, U. (1992). The 46/50 kDa phosphoprotein VASP purified from human platelets is a novel protein associated with actin filaments and focal contacts. EMBO J. *11*, 2063–2070.

Rottner, K., Behrendt, B., Small, J. V., and Wehland, J. (1999). VASP dynamics during lamellipodia protrusion. Nat. Cell Biol. *1*, 321–322.

Samarin, S., Romero, S., Kocks, C., Didry, D., Pantaloni, D., and Carlier, M. F. (2003). How VASP enhances actin-based motility. J. Cell Biol. *163*, 131–142.

Schafer, D. A., Welch, M. D., Machesky, L. M., Bridgman, P. C., Meyer, S. M., and Cooper, J. A. (1998). Visualization and molecular analysis of actin assembly in living cells. J. Cell Biol. *143*, 1919–1930.

Schirenbeck, A., Arasada, R., Bretschneider, T., Schleicher, M., and Faix, J. (2005). Formins and VASPs may co-operate in the formation of filopodia. Biochem. Soc. Trans. *33*, 1256–1259.

Schirenbeck, A., Arasada, R., Bretschneider, T., Stradal, T. E., Schleicher, M., and Faix, J. (2006). The bundling activity of vasodilator-stimulated phosphoprotein is required for filopodium formation. Proc. Natl. Acad. Sci. USA. *103*, 7694–7699.

Small, J. V. (1988). The actin cytoskeleton. Electron. Microsc. Rev. *1*, 155–174.

Svitkina, T. M., and Borisy, G. G. (1999). Arp2/3 complex and actin depolymerizing factor/cofilin in dendritic organization and treadmilling of actin filament array in lamellipodia. J. Cell Biol. *145*, 1009–1026.

Svitkina, T. M., Bulanova, E. A., Chaga, O. Y., Vignjevic, D. M., Kojima, S., Vasiliev, J. M., and Borisy, G. G. (2003). Mechanism of filopodia initiation by reorganization of a dendritic network. J. Cell Biol. *160*, 409–421.

Tilney, L. G., Connelly, P. S., and Guild, G. M. (2004). Microvilli appear to represent the first step in actin bundle formation in *Drosophila* bristles. J. Cell Sci. *117*, 3531–3538.

Vasioukhin, V., and Fuchs, E. (2001). Actin dynamics and cell-cell adhesion in epithelia. Curr. Opin. Cell Biol. *13*, 76–84.

Vignjevic, D., Kojima, S., Aratyn, Y., Danciu, O., Svitkina, T., and Borisy, G. G. (2006). Role of fascin in filopodial protrusion. J. Cell Biol. *174*, 863–875.

Vignjevic, D., Yarar, D., Welch, M. D., Peloquin, J., Svitkina, T., and Borisy, G. G. (2003). Formation of filopodia-like bundles in vitro from a dendritic network. J. Cell Biol. *160*, 951–962.

Walders-Harbeck, B., Khaitlina, S. Y., Hinssen, H., Jockusch, B. M., and Illenberger, S. (2002). The vasodilator-stimulated phosphoprotein promotes actin polymerisation through direct binding to monomeric actin. FEBS Lett. *529*, 275–280.

Waldmann, R., Nieberding, M., and Walter, U. (1987). Vasodilator-stimulated protein phosphorylation in platelets is mediated by cAMP- and cGMP-dependent protein kinases. Eur. J. Biochem. *167*, 441–448.

Zigmond, S. H. (2004). Formin-induced nucleation of actin filaments. Curr. Opin. Cell Biol. *16*, 99–105.

Zigmond, S. H., Evangelista, M., Boone, C., Yang, C., Dar, A. C., Sicheri, F., Forkey, J., and Pring, M. (2003). Formin leaky cap allows elongation in the presence of tight capping proteins. Curr. Biol. *13*, 1820–1823.

Zimmermann, J., Labudde, D., Jarchau, T., Walter, U., Oschkinat, H., and Ball, L. J. (2002). Relaxation, equilibrium oligomerization, and molecular symmetry of the VASP (336–380) EVH2 tetramer. Biochemistry *41*, 11143–11151.